

Article

Ultrasound-Assisted Extraction of β -Asarone from Sweet Flag (*Acorus calamus*) Rhizome

Noridayu Omer^{1,2}, Yeun-Mun Choo¹ , Muthupandian Ashokkumar^{3,*}  and Nor Saadah Mohd Yusof^{1,*} ¹ Department of Chemistry, Faculty of Science, Universiti Malaya, Kuala Lumpur 50603, Malaysia² Research Services Division (BPP), Institute of Research Management and Services (IPPP), Universiti Malaya, Kuala Lumpur 50603, Malaysia³ School of Chemistry, University of Melbourne, Parkville, VIC 3010, Australia

* Correspondence: masho@unimelb.edu.au (M.A.); adah@um.edu.my (N.S.M.Y.)

Abstract: In this study, the extraction efficiency of β -asarone from Malaysian *Acorus calamus* from Acoraceae family using conventional solvent extraction and ultrasound-assisted extraction techniques was compared. The results showed that the ultrasound-assisted extraction technique significantly improves the extraction yields and process feasibility without changing the structure of the active compound, i.e., β -asarone. The extraction yield increment was found to be ~2.5-fold and ~1.6-fold at 1:100 and 1:50 solid-to-solvent ratio, at 30% applied sonication power. The positive impact of sonication can also be observed for both mechanistic stages of extraction, i.e., the washing and diffusion stages, due to the favorable physical effect of acoustic cavitations. The observation was supported by the SEM images of the plant residue. The characterization of the extract was carried out using HPLC, NMR, UV and IR techniques. In conclusion, ultrasound assistance increases the extraction efficiency by ~2.5-fold even at only 30% applied ultrasonic power at a 1:100 solid-to-solvent ratio. The present study also provides an efficient and simple method for accurate direct dosing of *Acorus calamus* extracts to an application.



Citation: Omer, N.; Choo, Y.-M.; Ashokkumar, M.; Yusof, N.S.M.

Ultrasound-Assisted Extraction of β -Asarone from Sweet Flag (*Acorus calamus*) Rhizome. *Appl. Sci.* **2022**, *12*, 11007. <https://doi.org/10.3390/app12211007>

Academic Editor: Monica Gallo

Received: 2 September 2022

Accepted: 27 October 2022

Published: 30 October 2022

Publisher's Note: MDPI stays neutral with regard to jurisdictional claims in published maps and institutional affiliations.



Copyright: © 2022 by the authors. Licensee MDPI, Basel, Switzerland. This article is an open access article distributed under the terms and conditions of the Creative Commons Attribution (CC BY) license (<https://creativecommons.org/licenses/by/4.0/>).

Keywords: ultrasound assistance; asarone; HPLC; NMR; UV; IR; *Acorus calamus*

1. Introduction

Acorus calamus is commonly known as sweet flag, Bacha or Jerangau Putih [1]. Asarone is a naturally occurring phenylpropanoid usually found in the Acoraceae (*Acorus*) and Aristolochiaceae (*Asarum*) plant families [2–7]. All of its variations, the α -, β - and γ -asarone are commonly used in naturopathy due to their significant medicinal and pharmacological values [4,5,8,9]. Amongst the proven benefits of asarone is the treatment of various physiological disorders such as hyperlipidaemia, respiratory, circulation problems, neurological disorders, epilepsy, Alzheimer's and ischemia [3,5,10–12]. Asarone is also known to relieve inflammation and gas or colic, and treatment for diarrhea, ulcers and intestine-related issues. Moreover, asarone can act as an antidepressant, relaxant or calm inducer, thus helping with sleeping problems and minor psychological issues. Asarone provides quick relief due to its ability to cross the blood–brain barrier, thus directly affecting the body's central nervous system [13].

However, there are numerous reports on the concerns over the safety of asarone. It was reported that prolonged exposure to *A. calamus* could cause toxification and excessive vomiting [14]. It was also reported that both α - and β -asarone are cytotoxic, genotoxic and hepatocarcinogenic [12,15,16]. Due to the reported toxicity effects of asarones, the use of *A. calamus* in food and flavoring is prohibited by law in certain countries, including the United States of America [17]. Despite the decision of certain countries to refuse the use of asarone, there are an increasing number of studies that prove the benefits of the compound in treating various health issues. Therefore, instead of a complete ban, some countries introduce regulations that limit the intake of β -asarone [9,10,18–20]. Hence, it is important

to have an efficient and reliable method to determine accurately the amount of β -asarone in *A. calamus* to reduce the risk of toxication.

Ultrasound is known to aid the extraction process by increasing extract yield and improving the experimental feasibility. The phenomenon of microbubble oscillation and collapse causes the physical effect necessary to aid the extraction process. The oscillation of the microbubbles may result in macro turbulences that could improve solute in solvent micro-mixing. The event would also promote materials collision, thus fragmenting and rupturing the plant material structure. On the other hand, the collapse of the microbubble results in violent phenomena such as micro-jetting and shockwaves with extreme temperature and pressure released locally. Such occurrences on the plant surface result in the fragmentation and disruption of the material matrix, detachment and erosion of the sacs and glands, and sonoporation that could aid the release of its active compounds bound by the structure. Therefore, there have been many reports on the improved extraction efficiency by ultrasound aidance. The ultrasound-assisted extraction efficiency is also known to be affected by many experimental factors, such as material particle size [21,22] and moisture contents [23,24]; and ultrasound parameters such as frequency, power and sonication time [25,26].

Several studies on the extraction and quantification of asarone by HPTLC [27,28], HPLC [29], GCMS [30,31], LC-MS/MS [32–34] and near-infrared reflection (NIR) spectroscopy [35] have been reported. In this study, an ultrasound-assisted extraction coupled with HPLC analysis is developed to provide an efficient and simple method to quantify β -asarone in the *A. calamus*. The effects of experimental conditions such as the size of plant materials, solvent medium, and sonication power were investigated, while the ultrasound reactor design was kept constant. The extraction efficiency of the ultrasound assisted method was compared with the conventional solvent extraction method.

2. Materials and Methods

2.1. Plants Materials

In this study, dried rhizomes of *Acorus calamus* were obtained from Alor Setar, Kedah, Malaysia. The rhizomes were ground to particles with size ranges from 0.05 to 0.20 cm for extraction.

2.2. Conventional Solvent Extraction of *A. calamus*

The processes involved during the extraction are depicted in Figure 1. An amount of 0.5 or 1.0 g of ground *A. calamus* was soaked in a container with 50 mL of ethanol (purity of $\geq 95\%$ from Kofa Chemicals) for 30 min in a condition of with and without temperature control. This makes the solid-to-solvent ratios to be either at 1:100 or 1:50 (g/mL). The temperature was maintained using a water bath coupled with a thermoregulator at 40–45 °C. After the extraction, the ethanol extract was filtered through a 0.45 μ m nylon membrane filter (Millipore HNWP04700). The ethanol solvent in the filtrate was then removed under reduced pressure and the dried crude extract was stored at room temperature. The experiment was performed in triplicates. Isolation and purification were extensively carried out on the crude extract using column chromatography (CC; 10 g silica gel 60, 0.040–0.063, Merck, Darmstadt, Germany; chloroform:hexane (1:1), 500 mL) and centrifugal thin layer chromatography (CTLC; Silica gel 60 PF₂₅₄ containing gypsum, Merck, Darmstadt, Germany, 2 mm thick; chloroform:hexane (1:1), 250 mL). Both techniques were repeated until a single spot in TLC was obtained. The purified β -asarone was then characterized using NMR, IR and UV-spectroscopy for identification confirmation. The extracted ground rhizome was air-dried for microscopy analysis. The extraction process was carried out in a fume hood. However, throughout the processes, the strong distinct smell of β -asarone can be immediately detected and lingers. Mask and gloves were used during the whole extraction process to reduce the risk of β -asarone intoxication.

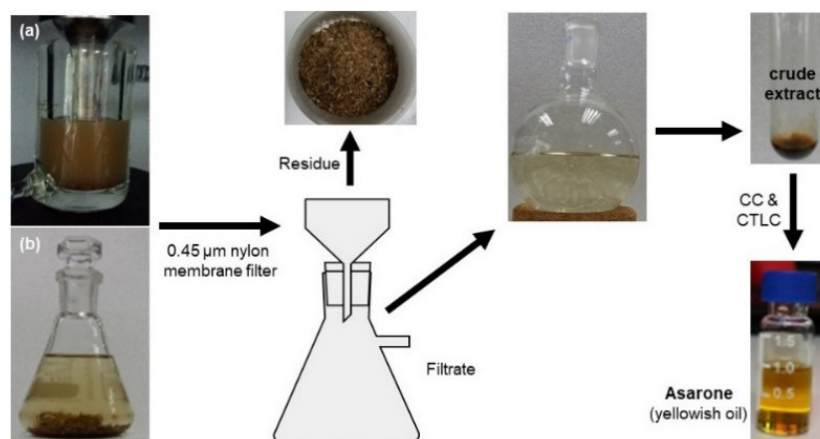


Figure 1. The (a) ultrasonic-assisted and (b) conventional solvent extraction processes in obtaining the pure asarone from *A. calamus* rhizome.

2.3. Ultrasonic-Assisted Extraction of *A. calamus*

The ultrasonic-assisted extraction was carried out for similar solvent volume, time, replication and solid-to-solvent ratio as the conventional solvent extraction method. The ultrasound unit used was a 20 kHz ultrasonic probe (Qsonica Q500, Qsonica LLC., Newton, NJ, USA) with a tip diameter of 1.0 cm. The probe was immersed and maintained at 1.0 cm below the solvent surface throughout all experiments. This is shown in Figure 1a above. The sonication power was varied at 30, 5, and 70% with power densities of 471.2 Wdm^{-3} , 981 Wdm^{-3} , and 1571.6 Wdm^{-3} , respectively. The subsequent processes are similar to the conventional method.

2.4. Characterization

The NMR spectra data were obtained from a 400 MHz Bruker AVANCE III spectrometer with chemical shifts (δ) expressed in ppm and TMS as an internal standard in CDCl_3 . The coupling constants (J) are reported in Hz. The UV measurement was carried out using ethanol solvent with UV-Vis spectrophotometer (Shimadzu, UV-1800, Shimadzu Corporation, Kyoto, Japan). The IR measurement was carried out on the Perkin-Elmer RX1 FT-IR (Perkin Elmer, Waltham, MA, USA) spectrophotometer using the thin film method with NaCl cell. HRMS data were obtained from an Agilent 6530 Q-TOF (Agilent Technologies, Santa Clara, CA, USA) mass-spectrometer coupled with an Agilent 1200 series Rapid Resolution LC system (Agilent Technologies, Santa Clara, CA, USA). All characterization was performed with the extracted β -asarone.

The physical structures of the rhizomes before and after being treated with both ultrasound-assisted and conventional extraction were observed under a field emission scanning electron microscope (FESEM, Hitachi SU8220, Hitachi High-Tech Corporation, Tokyo, Japan). Samples were uncoated and observed under 1 kV.

2.5. HPLC Analysis

The kinetic study of the extraction process was carried out using HPLC to quantify the amount of β -asarone from the extracts obtained from Section 2.2, while the calibration curve was constructed using the purified β -asarone in the present study. The compound was dissolved in 1.5 mL of methanol (HPLC grade) and passed through a $0.45 \mu\text{m}$ membrane filter. HPLC analysis was performed on Agilent's HPLC system equipped with 1290 Infinity Binary pump and autosampler injector, Agilent Poroshell 120 C18 column ($4.6 \times 50 \text{ mm}$, $2.7 \mu\text{m}$), and PDA detector. Sample volume was $1 \mu\text{L}$ and eluted using mobile phase of methanol: MiliQ water (90:10, v/v), delivered at a flow rate of 0.4 mL/min . Detection was carried out at 260 nm. The analysis was carried out in triplicates. The HPLC spectrum of β -asarone at 260 nm is shown in Figure 2. A calibration curve of the pure β -asarone was

developed with its concentration range of 10–200 $\mu\text{g}/\text{mL}$ (Figure S1 of SI). The calibration curve was used to determine the extract yield (Y_t). The Y_t data were subsequently used for kinetic modelling calculation.

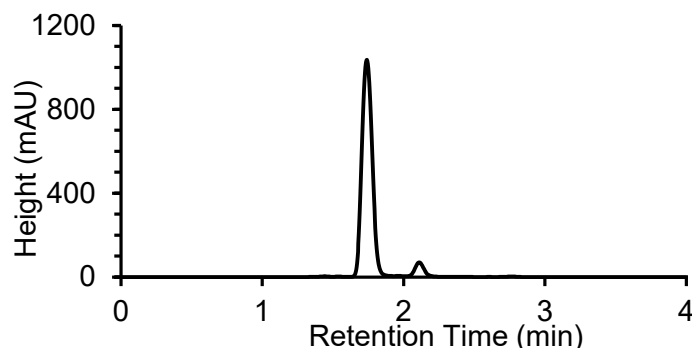


Figure 2. The HPLC spectrum of β -asarone (1.7 min; >95% purity).

2.6. Kinetic Modeling

The β -asarone extraction progress plot was fitted according to the So and MacDonald's model [36]. The kinetics equation that describes the extraction process is given as Equation (1).

$$Y_t = c_w [1 - e^{-k_w t}] + c_d [1 - e^{-k_d t}] \quad (1)$$

where Y_t is the amount of solute extracted at any given time ($\mu\text{g}/\text{mL}$), c_w is the amount of solute extracted in the solvent during the washing step, k_w is the rate of extraction during the washing step (min^{-1}), c_d is the amount of solute extracted in the solvent during the diffusion step and k_d is the rate of extraction during the diffusion step (min^{-1}). All experiments were performed in triplicates and the results were expressed as mean value \pm standard deviation. The statistical analysis of the model was carried out using JMP 15 and Excel 2016.

3. Results and Discussions

3.1. Characterization of β -Asarone

In this study, the extraction of the volatile β -asarone oil was carried out from the *A. calamus* rhizomes using two techniques—the conventional solvent extraction and ultrasound-assisted extraction techniques (Figure 1a,b). The major component of the extract and the focus of this study, β -asarone or 1,2,4-trimethoxy-5-(prop-1-en-1-yl)benzene is shown below in Figure 3a. The UV spectrum showed three absorption maxima at 302, 252 and 203 (Figure 3b). The IR spectrum indicated the presence of methyl group C-H stretch (2936 cm^{-1}), aromatic ring C-C stretch (1608 , and 1508 cm^{-1}) and ether C-O stretch (1203 cm^{-1}) functional groups (Figure 3c). The m/z is found to be $209.0954 [\text{M}+\text{H}]^+$ (calcd. 209.1172) (Figure 3d).

The purified β -asarone was further characterized by ^1H and ^{13}C NMR spectra. Both spectra are shown in Figure 4. The ^1H NMR spectrum displayed eight proton signals. Of the eight proton signals, two signals were observed as a doublet of doublet (dd) at δH 6.46 and 1.82, one signal was observed as multiplet (m) at δH 5.74 and the other five signals were observed as singlet (s) at δH 6.82, 6.51, 3.87, 3.81 and 3.78. The COSY, DEPT, HSQC and HMBC spectra are provided as Figures S2 to S5 in the SI. The COSY spectrum indicated the partial structure $-\text{CH}=\text{CH}-\text{CH}_3$, corresponding to C(7)-C(8)-C(9), hence suggesting the presence of the aliphatic chain substituted at the aromatic rings system. The ^{13}C NMR spectrum showed the presence of an sp^3 primary carbon, three sp^3 methoxy carbon, four sp^2 tertiary carbon and four sp^2 quaternary carbon signals. The carbon signals at δC 56.12, 56.50 and 56.66 indicated the presence of three methoxy carbon, while the δH 14.70 suggested the presence of an sp^3 primary carbon. The experimental spectroscopic data (NMR, UV, IR and MS) of β -asarone are similar to the values from the literature [7].

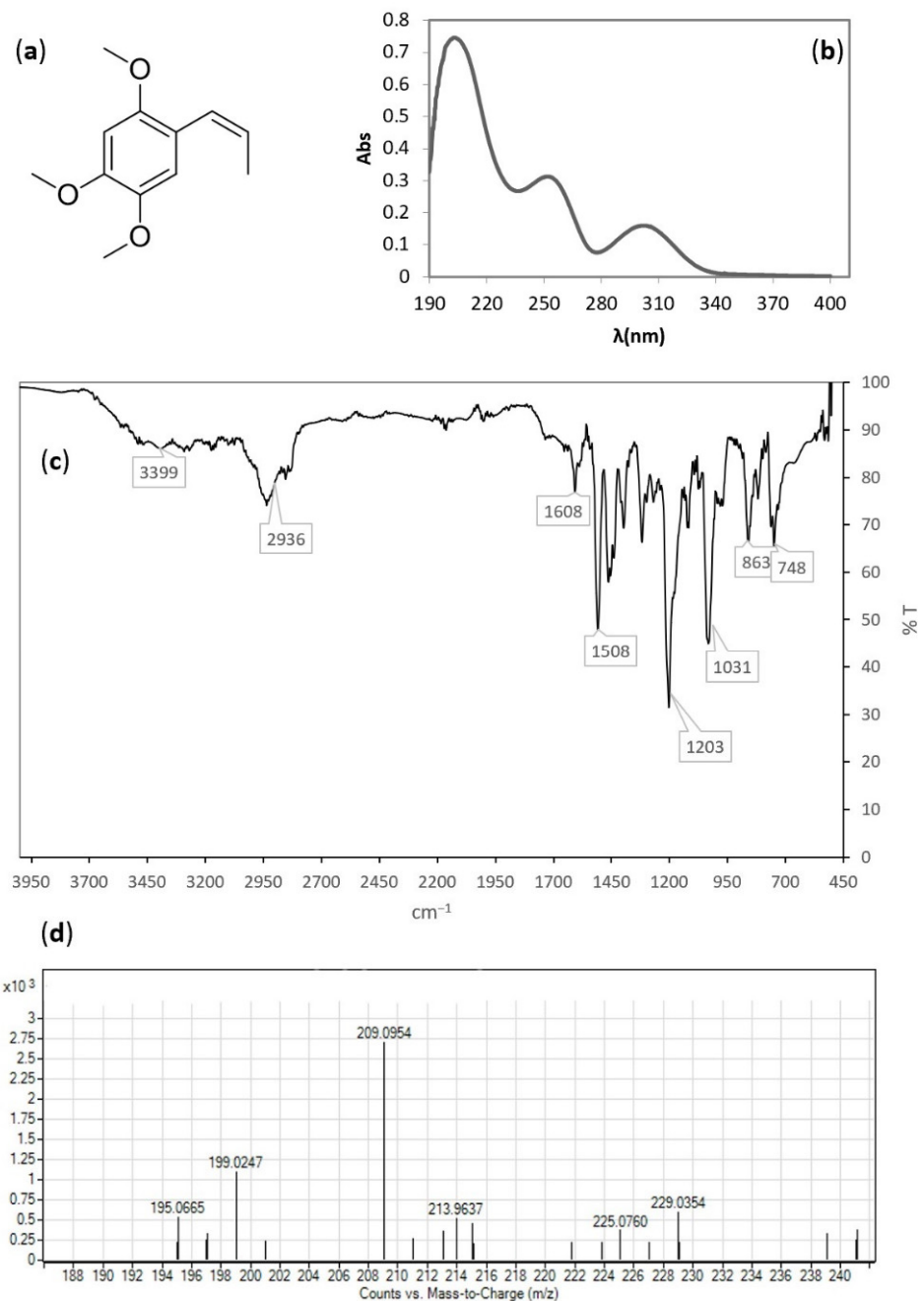


Figure 3. (a) The chemical structure, (b) UV, (c) IR and (d) HRMS spectra of β -asarone.

The HPLC spectrum of β -asarone at 260 nm (Figure 2) showed two peaks at 1.7 and 2.1 min. The characterization of purified β -asarone is crucial as it is used as a reference for the kinetics study.

3.2. The Kinetics of Ultrasonic-Assisted Extraction of *A. calamus*

The ultrasound-assisted extraction was carried out to improve the extraction of β -asarone from *A. calamus*. The increasing β -asarone yield of extraction upon sonication duration of 30 min for 1:100 and 1:50 solid-to-solvent ratios are shown in Figures 5 and 6, respectively for sonication power of 30 (Δ), 50 (\times), 70% (\square); and in the absence of sonication, with the presence of temperature (\circ) and without (\diamond). The extract yield was calculated from the calibration curve of the purified β -asarone constructed using HPLC technique as

shown in Figure S1 in SI. The lines in the figures were plotted with the calculated values modelled according to Equation (1).

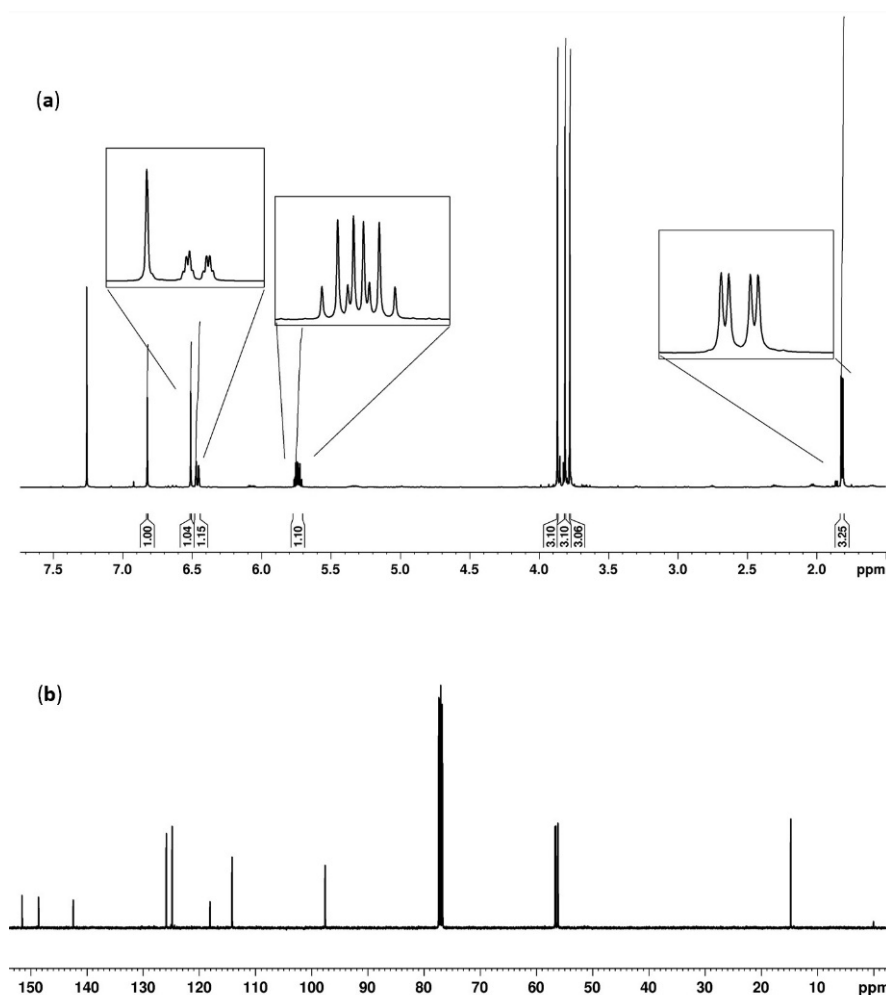


Figure 4. (a) $^1\text{H-NMR}$ (CDCl_3 , 400 MHz) and (b) $^{13}\text{C-NMR}$ (CDCl_3 , 100 MHz) spectra of asarone.

The extraction progress plots revealed the typical trend of the extraction curve commonly observed. The curves are described by the two important mechanistic stages during extraction—the washing and diffusion mechanism [36]. Washing refers to the initial stage of extraction where the volatile oil is relatively easier to be washed out and is usually characterized by the rapid increase in the extraction plot. The high rate of extraction is due to the location of the active compounds at various sites of the plant matrices. As the samples are soaked in the medium, the solvent pervades into the plant matrices and solubilized the easily accessible solutes, washing them out. The affected solutes in this stage are those located near the surface or originally adsorbed on the surface of the matrices. Therefore, the more compounds available on the surface, the higher the rate of the washing mechanism. On the other hand, the solutes located in the interior or enclosed within the structure of the plant matrices will only be diffused out by the solvent diffusion process. The diffusion process represents the later stage of the extraction plot where the increment of extract yield happens at a slower rate, even though the two stages in the mechanism work in different manners, simultaneously. Thus, the two processes cannot be completely distinguished in the discussion. However, the domination of one process over the other is clearly evident in the plots shown in Figures 5 and 6. The rapid increase in yield extract within \sim the first 10 min of the extraction indicates the dominance of the washing stage

over the diffusion stage, whilst the slow increment of the extract yield that follows indicates the dominance of the diffusion stage over the washing stage.

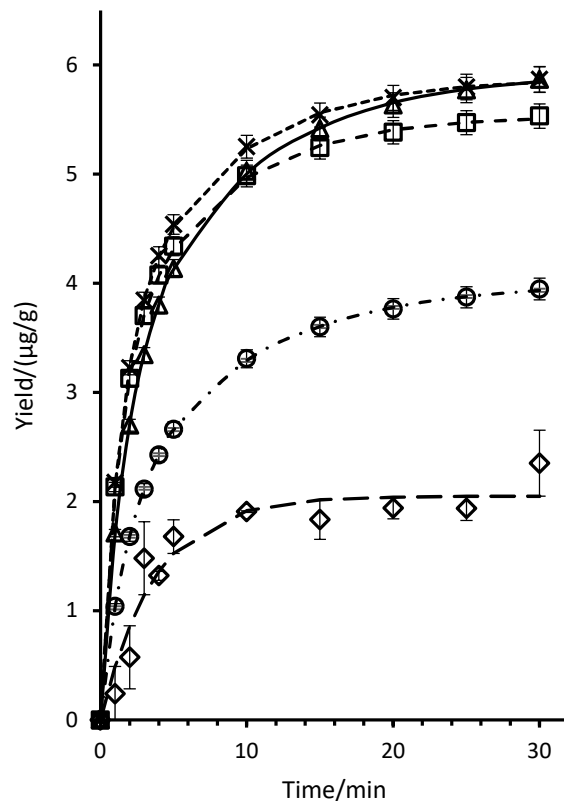


Figure 5. The extraction progress plot of β -asarone at solid-to-solvent ratio 1:100 with sonication power of 70 (\square), 50 (\times), 30% (Δ), and in the absence of sonication, with the presence of temperature (\odot) and without (\diamond). The lines were plotted with the calculated value according to Equation (1) for sonication power of 70 (dashed line), 50 (dotted line), 30% (straight line), and in the absence of sonication with the presence of temperature (dash-dot line) and without (long dashed line).

To kinetically explain the β -asarone extraction yield during the washing and diffusion stages, the progress of extraction is fitted to the So and MacDonald's model as shown in Equation (1). The washing rate coefficient is kinetically depicted by k_w values, and the diffusion rate coefficient is depicted by k_d values. The extract yield, Y_t of the extraction in the presence and absence of ultrasound aid is also shown in Table 1 below.

Before we delve into the effect of ultrasound assistance, a quick look at the extract yield in Table 1 showed a higher amount of extract yield at 1:50 as compared to the 1:100 solid-to-solvent ratio. This indicates that extracting 1.0 g of *Acorus calamus* in 50 mL of ethanol is practical even though it was initially doubted during the experiment. This is because it is known that a larger solid-to-solvent ratio results in a higher concentration gradient, thus allowing more solvent penetration into the material [37]. Therefore, the lower amount of ground *A. calamus*, the higher surface contact between plant material, and hence the greater the improvement of the extraction yields. The larger amount of β -asarone extracted at a higher solid-to-solvent ratio (1:50) proved that having 1.0 g of ground *A. calamus* in 50 mL of ethanol is efficient and suitable for further investigation in this study. It is also notable to mention that β -asarone has good solubility in ethanol at 50 mg/mL [38]. A higher solid-to-solvent ratio effect than 1:50 was not explored in this study.

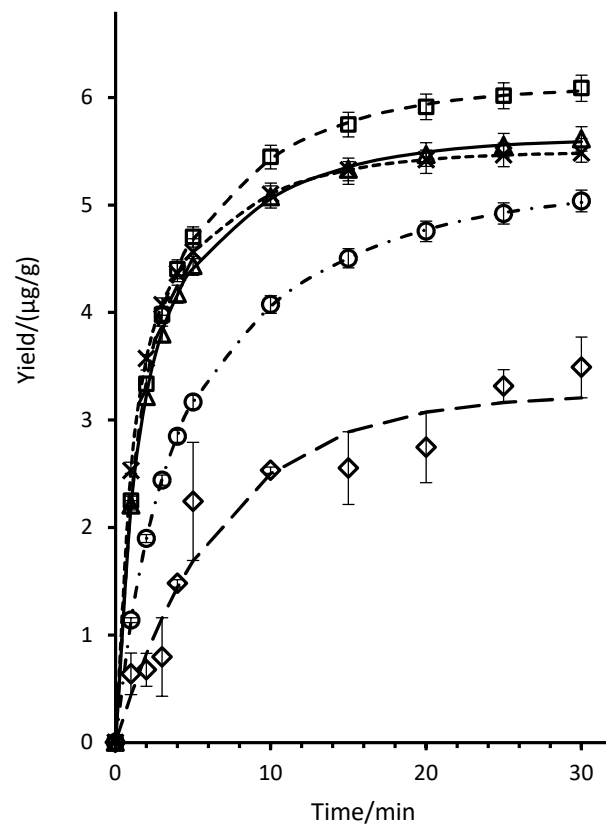


Figure 6. The extraction progress plot of β -asarone at solid-to-solvent ratio 1:50 with sonication power of 70 (\square), 50 (\times), 30% (Δ), and with the presence of temperature (\circ) and without (\diamond). The lines were plotted with the calculated value according to Equation (1) for sonication power of 70 (dashed line), 50 (dotted line), 30% (straight line), and in the absence of sonication with the presence of temperature (dash-dot line) and without (long dashed line).

Table 1. The extract yield, Y_t of the extraction in the presence and absence of ultrasound. The values of c_w , k_w , c_d and k_d .

Solid-to-Solvent Ratio (g:mL)	Sonication Power ^c (%)	Extract Yield	c_w	$10^3 k_w$	c_d	$10^3 k_d$
		^f Y_t ($\mu\text{g/g}$)				
1:100 ^a	30	5.869 ± 0.024	2.860 ± 0.128	633 ± 28	3.071 ± 0.110	120 ± 6
	50	5.867 ± 0.029	3.222 ± 0.132	816 ± 36	2.657 ± 0.116	142 ± 9
	70	5.532 ± 0.029	3.099 ± 0.125	852 ± 39	2.439 ± 0.111	146 ± 10
	^d 0 _T	3.948 ± 0.015	1.833 ± 0.086	569 ± 25	2.179 ± 0.073	112 ± 6
	^e 0	2.352 ± 0.015	2.049 ± 0.109	273 ± 49	n.a.	n.a.
1:50 ^b	30	5.617 ± 0.030	3.176 ± 0.128	870 ± 40	2.444 ± 0.114	148 ± 10
	50	5.511 ± 0.033	3.378 ± 0.135	1055 ± 52	2.120 ± 0.122	168 ± 14
	70	6.089 ± 0.031	3.338 ± 0.136	813 ± 136	2.765 ± 0.120	141 ± 9
	^d 0 _T	5.039 ± 0.015	2.182 ± 0.111	485 ± 21	2.992 ± 0.092	100 ± 5
	^e 0	3.491 ± 0.015	3.245 ± 0.207	148 ± 27	n.a.	n.a.

n.a.—Not available; ^a 0.5 g of ground *A. calamus* in 50 mL of ethanol; ^b 1.0 g of ground *A. calamus* in 50 mL of ethanol; ^c The power percentage from the total power of 500 W ultrasonic unit; ^d The extraction was carried out in the absence of ultrasound assistance at 40–45 °C; ^e The extraction was carried out in the absence of ultrasound assistance at ambient temperature; ^f The yield of β -asarone per gram of *A. calamus*.

That the extract yields (Y_t) of the 1:50 conventional experiments are higher than that of 1:100 conventional is due to a larger amount of *A. calamus* being used in the 1:50 experiment (1.0 g) than the 1:100 experiment (0.5 g). It is also interesting to note that the k_w of both

heated and non-heated 1:50 and 1:100 experiments are very low, while the k_d value for non-heated conventional extraction was too low for determination. This shows that in non-heated conventional extraction, the extraction process was in the washing stages in which β -asarone was extracted slowly from the plant surface. As expected, heated non-conventional extraction increases the extract yields (Y_t) when compared to the non-heated experiments, i.e., ~ 1.7 -fold for 1:100 and ~ 1.4 -fold for 1:50 experiments. However, caution needs to be exercised for heated conventional extraction as β -asarone is known to be volatile.

The extraction yields of (Y_t) Increase substantially when sonication power was applied for all experiments. The largest increase (2.5-fold) was observed in the 30% sonication power to 1:100 solid-to-solvent ratio experiment. This shows the advantages of applying sonication in the extraction process.

The results in Table 1 showed a slight increase in extract yield (Y_t) (30% and 50% ultrasound power) in the solid-to-solvent ratio 1:100 experiment when compared to that of the 1:50 experiment, indicating the dominant effect of a higher concentration gradient due to lower solid-to-solvent ratio [37]. However, at 70% ultrasound power, the higher solid-to-sample ratio experiment (1:50) gave a higher extraction yield, indicating the favorable application of ultrasound-assisted extraction in a higher solid-to-solvent ratio. However, it was observed that the variation in ultrasound power does not exert much difference on the extraction yield. This observation proves that efficient energy processing can be achieved even at low sonication power for small-scale extraction of β -asarone from *A. calamus*.

Using the kinetic model as represented in Equation (1), we can further analyze the effect of sonication upon the washing- and diffusion-dominance stages of extraction. It was interesting to note that for the 1:100 solid-to-solvent ratio, the rate of washing stage (k_w) increment was very dependent on the sonication power used. The increments were ~ 1.5 -fold ($852/569 \times 10^{-3}$), ~ 1.4 -fold ($816/569 \times 10^{-3}$) and ~ 1.1 -fold ($633/569 \times 10^{-3}$) for 70%, 50% and 30% ultrasound power applied, respectively. The same trend was observed for the 1:50 solid-to-solvent ratio condition with increments of ~ 1.6 ($815/485 \times 10^{-3}$), ~ 2.2 ($1055/485 \times 10^{-3}$), and ~ 1.8 ($870/485 \times 10^{-3}$) for 70, 50 and 30% ultrasound power applied, respectively. Such observation implies the significant ultrasound influence on the washing stage during the extraction process. Further discussion on the physical effect of sonication on the washing mechanistic stage will be presented in the following section.

A similar trend was observed for the rates of diffusion stage (k_d). For the 1:100 solid-to-solvent ratio, the k_d were found to increase by ~ 1.3 -fold ($146/112 \times 10^{-3}$), ~ 1.3 -fold ($142/112 \times 10^{-3}$) and ~ 1.1 -fold ($120/112 \times 10^{-3}$) for 70, 50 and 30% ultrasound power applied, respectively. For the 1:50 solid-to-solvent ratio, the k_d were found to increase by ~ 1.4 -fold ($141/100 \times 10^{-3}$), ~ 1.7 -fold ($168/100 \times 10^{-3}$), and ~ 1.5 -fold ($148/100 \times 10^{-3}$) for 70, 50, and 30% ultrasound power applied, respectively. This could also represent the ability of ultrasound to positively influence the diffusion process.

3.3. The Physical Effect of Sonication in UAE

The extract of the ultrasound-assisted process was subjected to isolation, purification and characterization similar to the extract from conventional solvent extraction. The extraction product including β -asarone was found to be the same, confirming that the ultrasound process does not change any of the compound structure. Therefore, it is safe to deduce the qualitative characteristics of *A. calamus* extract, including its biochemical activity is impervious to ultrasound irradiation in this study. The significant efficiency increase in the extraction is due to the physical effect of sonication.

There have been many reports on the physical effect of ultrasonication during the extraction process [26,39–41]. In this study, similar effects were observed from the SEM images. The dried *A. calamus* rhizomes (Figure 7a) were ground to uniform sizes as shown in Figure 7b. The SEM images of the ground samples are shown in Figure 7c,d with their usual matrix characteristics such as fibers secretion, and oil sacs. The active compounds of

the plants are available on the surface or exterior of the matrices, as well as enveloped in the oil sacs.

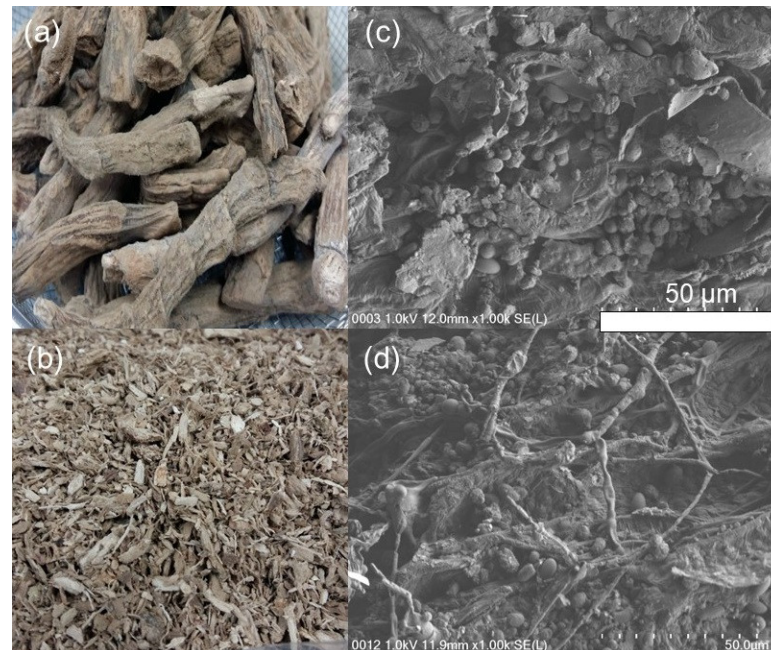


Figure 7. The (a) dried and (b) ground *A. calamus* samples. (c,d) are the plant matrices with visible structures of fiber and oil glands at 1000 \times magnification.

During the solvent extraction process, the active compounds available on the plant matrices are extracted mostly via the washing mechanism, whilst the active compounds in the oil sacs are extracted by the process of diffusion. This is clearly visible in the SEM images of the *A. calamus* residue after solvent extraction, as shown in Figure 8. The secretion or oil glands are now depleted and flattened. The diffusion process induced by the solvent has caused the sacs to be emptied. However, the plant structures are still well intact, without any significant rupture or damage.

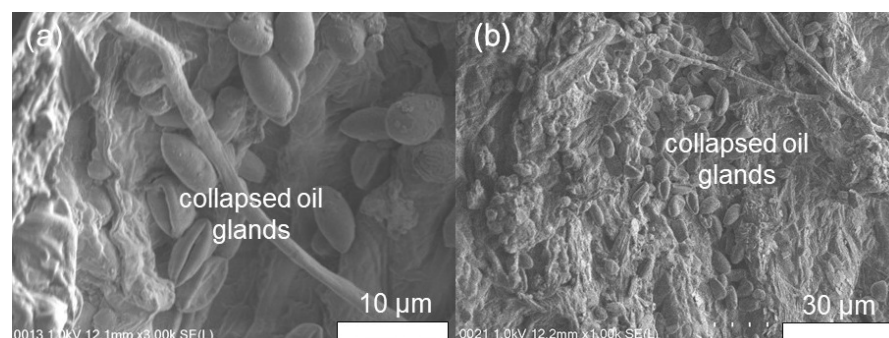


Figure 8. The SEM images of the *A. calamus* residue after the solvent extraction process. Both images (a) and (b) shows the collapsed oil glands at different magnifications after the active compound is extracted. Image (a) was taken at 3000 \times magnification and image (b) at 1000 \times magnification.

The SEM images of plant residue upon ultrasound-assisted extraction were also taken to compare the impact of sonication on the plant structure. By a quick look at the four images in Figure 9 and comparing them to the images in Figures 7 and 8, it can be clearly seen that the plant structures are heavily impacted by the process of sonication. Sonication results in acoustic cavitation, in which the formation and growth was by rectified diffusion, and the collapse of microbubbles. The process leads to high shear forces in the

media. The implosion of microbubbles on a plant matrix results in micro jetting which generates effects such as particle breakdown or formation of pores [39]. Many of the cell walls are ruptured, therefore also breaking the sacs and cells. The strong agitation from microbubble oscillation and implosion could result in the fragmentation of the structures into smaller pieces, thus increasing the surface areas for contact with the solvent, thus improving the extraction efficiency. The damages of sonofragmentation effect can be seen in all four pictures; an example is in Figure 9a. Sonofragmentation effect can be seen resulting from bubble collapse, as well as the collision of the particles during ultrasound-induced streaming. The surface of the plant matrix had also been eroded by the physical action of ultrasound, as seen in Figure 9b. The visible impact of erosion is due to the release of solid structures into the solvent [26]. These are among the physical impacts of sonication that increase the extraction during the washing mechanism by decreasing the diffusion boundary, thus accelerating mass transfer to the solvent phase [42]. The effect of sonoporation can also be seen in Figure 9c. The pores formed are due to the microbubble implosion on the surface of the structure. The pores will increase the membrane permeability, which in turn discharges the active compounds [43]. The ultrasound-induced maceration is also evident in Figure 9d. The sacs were seen to be attached at the surface of the rhizome but pushed deeper into the surrounding structure. The ultrasound-induced maceration is caused when the microjet generation from microbubble implosion jets directly towards the sacs, thus pushing the sac deeper, yet, releasing the oil into the surrounding [44].

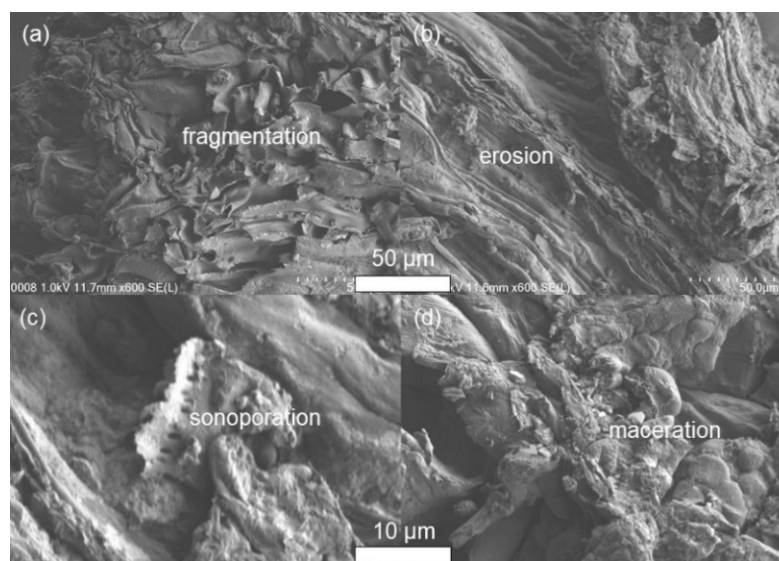


Figure 9. The SEM images of the *A. calamus* residue after the ultrasound-assisted extraction process. The images are evidence of physical impact from ultrasound due to (a) fragmentation, (b) erosion, (c) sonoporation and (d) ultrasound-induced maceration.

The assistance of ultrasound also happens at a bigger scale. The oscillation of the microbubbles results in microstreaming which causes turbulence and disruptions to the solid samples, thus facilitating the mixing around the solvent, as well as enhancing the mass transfer [39]. The alternating compression and rarefaction ultrasound waves will also induce a sponge effect on the system. Apart from that, the implosion of the microbubbles will also increase the temperature during extraction. This mimics and improves the necessary factor as in the conventional solvent extraction.

4. Conclusions

In this study, β -asarone was successfully extracted from a species of *A. calamus* found in the northern part of Malaysia. The extraction was carried out using two techniques—the conventional solvent and ultrasound-assisted extraction at different solid-to-solvent ratios

and sonication powers. The extraction yields were quantified using the HPLC technique. The results allowed detailed quantitative analysis of the naturally occurring β -asarone, as well as providing a foundation for the evaluation of the two extraction techniques' efficiency. It was found that sonication can improve extraction efficiency and processing feasibility even at low power. The chemical structure of β -asarone was not affected by the sonification process, thus preserving the benefits of the compound β -asarone.

Supplementary Materials: The following supporting information can be downloaded at: <https://www.mdpi.com/article/10.3390/app122111007/s1>, Figure S1: Calibration curve of the pure β -asarone; Figure S2: COSY Spectrum of β -asarone; Figure S3: DEPT-135 Spectrum of β -asarone; Figure S4: HSQC Spectrum of β -asarone; Figure S5: HMBC Spectrum of β -asarone.

Author Contributions: Conceptualization, N.S.M.Y. and M.A.; methodology, N.O.; formal analysis, N.O.; investigation, N.O.; resources, N.S.M.Y. and Y.-M.C.; writing—original draft preparation, N.O. and N.S.M.Y.; writing—review and editing, N.S.M.Y.; supervision, N.S.M.Y. and Y.-M.C.; project administration, N.S.M.Y.; funding acquisition, N.S.M.Y. All authors have read and agreed to the published version of the manuscript.

Funding: This study was supported by grant from the Ministry of Higher Education under the Fundamental Research Grant Scheme (FRGS/1/2019/STG07/UM/02/2) and N.O. acknowledges the Ministry of Higher Education Malaysia for the MyBrain15 scholarship.

Institutional Review Board Statement: Not applicable (studies not involving humans or animals).

Informed Consent Statement: Not applicable.

Data Availability Statement: Data can be provided upon request to the corresponding author.

Conflicts of Interest: The authors declare no conflict of interest.

References

1. Seidemann, J. *World Spice Plants: Economic Usage, Botany, Taxonomy*; Springer: Berlin/Heidelberg, Germany, 2005.
2. Gao, E.; Zhou, Z.Q.; Zou, J.; Yu, Y.; Feng, X.L.; Chen, G.D.; He, R.R.; Yao, X.S.; Gao, H. Bioactive Asarone-Derived Phenylpropanoids from the Rhizome of *Acorus tatarinowii* Schott. *J. Nat. Prod.* **2017**, *80*, 2923. [[CrossRef](#)] [[PubMed](#)]
3. Yang, Y.X.; Chen, Y.T.; Zhou, X.J.; Hong, C.L.; Li, C.Y.; Guo, J.Y. Beta-asarone, a major component of *Acorus tatarinowii* Schott, attenuates focal cerebral ischemia induced by middle cerebral artery occlusion in rats. *BMC Complement. Altern. Med.* **2013**, *13*, 236. [[CrossRef](#)] [[PubMed](#)]
4. Zuba, D.; Byrska, B. Alpha- and beta-asarone in herbal medicinal products. A case study. *Forensic Sci. Int.* **2012**, *223*, e5–e9. [[CrossRef](#)] [[PubMed](#)]
5. Rajput, S.B.; Tonge, M.B.; Karuppaiyil, S.M. An overview on traditional uses and pharmacological profile of *Acorus calamus* Linn. (Sweet flag) and other *Acorus* species. *Phytomedicine* **2014**, *21*, 268–276. [[CrossRef](#)] [[PubMed](#)]
6. Uebel, T.; Hermes, L.; Hauptenthal, S.; Müller, L.; Esselen, M. α -Asarone, β -asarone, and γ -asarone: Current status of toxicological evaluation. *J. Appl. Toxicol.* **2021**, *41*, 1166–1179. [[CrossRef](#)]
7. Park, C.H.; Kim, K.H.; Lee, I.K.; Lee, S.Y.; Choi, S.U.; Lee, J.H.; Lee, K.R. Phenolic constituents of *Acorus gramineus*. *Arch. Pharmacol Res.* **2011**, *34*, 1289–1296. [[CrossRef](#)]
8. Chellian, R.; Pandey, V.; Mohamed, Z. Pharmacology and toxicology of α - and β -Asarone: A review of preclinical evidence. *Phytomedicine* **2017**, *32*, 41–58. [[CrossRef](#)]
9. Das, B.K.; Swamy, A.H.M.V.; Koti, B.C.; Gadad, P.C. Experimental evidence for use of *Acorus calamus* (asarone) for cancer chemoprevention. *Heliyon* **2019**, *5*, e01585. [[CrossRef](#)]
10. Geng, Y.; Li, C.; Liu, J.; Xing, G.; Zhou, L.; Dong, M.; Li, X.; Niu, Y. Beta-asarone improves cognitive function by suppressing neuronal apoptosis in the beta-amyloid hippocampus injection rats. *Biol. Pharm. Bull.* **2010**, *33*, 836–843. [[CrossRef](#)]
11. Fu, S.Y.; Fang, R.M.; Fang, G.L.; Xie, Y.H.; Fang, Y.Q. Effects of beta-asarone on expression of FOS and GAD65 in cortex of epileptic rat induced by penicillin. *J. Chin. Med. Mater.* **2008**, *31*, 79–81.
12. Qi, H.; Chen, L.; Ning, L.; Ma, H.; Jiang, Z.; Fu, Y.; Li, L. Proteomic analysis of β -asarone induced cytotoxicity in human glioblastoma U251 cells. *J. Pharm. Biomed. Anal.* **2015**, *115*, 292–299. [[CrossRef](#)]
13. Meng, X.; Liao, S.; Wang, X.; Wang, S.; Zhao, X.; Jia, P.; Pei, W.; Zheng, X.; Zheng, X. Reversing P-glycoprotein-mediated multidrug resistance in vitro by α -asarone and β -asarone, bioactive cis–trans isomers from *Acorus tatarinowii*. *Biotechnol. Lett.* **2014**, *36*, 685–691. [[CrossRef](#)]
14. Björnstad, K.; Helander, A.; Hultén, P.; Beck, O. Bioanalytical investigation of asarone in connection with *Acorus calamus* oil intoxications. *J. Anal. Toxicol.* **2009**, *33*, 604–609. [[CrossRef](#)]

15. Hasheminejad, G.; Caldwell, J. Genotoxicity of the alkenylbenzenes alpha- and beta-asarone, myristicin and elimicin as determined by the UDS assay in cultured rat hepatocytes. *Food Chem. Toxicol.* **1994**, *32*, 223–231. [[CrossRef](#)]
16. Unger, P.; Melzig, M.F. Comparative study of the cytotoxicity and genotoxicity of alpha- and Beta-asarone. *Sci. Pharm.* **2012**, *80*, 663–668. [[CrossRef](#)]
17. US Government Printing Office. Title 21, Food and Drugs, 21CFR189.110. In *Code of Federal Regulations*; US Government Printing Office: Washington, DC, USA, 2019.
18. Scientific Committee on Food, E.C. *Opinion of the Scientific Committee on Food on the Presence of β -Asarone in Flavorings and Other Food Ingredients with Flavoring Properties (SCF/CS/FLAV/FLAVOUR/9 ADD1 Final)*; European Medicines Agency (EMA): Brussels, Belgium, 2002.
19. Patel, D.N.; Ho, H.K.; Tan, L.L.; Tan, M.M.; Zhang, Q.; Low, M.Y.; Chan, C.L.; Koh, H.L. Hepatotoxic potential of asarones: In vitro evaluation of hepatotoxicity and quantitative determination in herbal products. *Front. Pharmacol.* **2015**, *6*, 25. [[CrossRef](#)]
20. Committee on Herbal Medicinal Products. *Public Statement on the Use of Herbal Medicinal Products Containing Asarone (EMA/HMPC/139215/2005)*; European Medicines Agency (EMA): London, UK, 2005.
21. Lorenzo, J.M.; Agregán, R.; Munekata, P.E.S.; Franco, D.; Carballo, J.; Şahin, S.; Lacombe, R.; Barba, F.J. Proximate Composition and Nutritional Value of Three Macroalgae: *Ascophyllum nodosum*, *Fucus vesiculosus* and *Bifurcaria bifurcata*. *Mar. Drugs* **2017**, *15*, 360. [[CrossRef](#)]
22. Dang, T.T.; Van Vuong, Q.; Schreider, M.J.; Bowyer, M.C.; Van Altena, I.A.; Scarlett, C.J. Optimisation of ultrasound-assisted extraction conditions for phenolic content and antioxidant activities of the alga *Hormosira banksii* using response surface methodology. *J. Appl. Phycol.* **2017**, *29*, 3161–3173. [[CrossRef](#)]
23. Stramarkou, M.; Papadaki, S.; Kyriakopoulou, K.; Krokida, M. Effect of drying and extraction conditions on the recovery of bioactive compounds from *Chlorella vulgaris*. *J. Appl. Phycol.* **2017**, *29*, 2947–2960. [[CrossRef](#)]
24. Dang, T.T.; Vuong, Q.V.; Schreider, M.J.; Bowyer, M.C.; Altena, I.A.V.; Scarlett, C.J. The Effects of Drying on Physico-Chemical Properties and Antioxidant Capacity of the Brown Alga (*Hormosira banksii* (Turner) Decaisne). *J. Food Process. Preserv.* **2017**, *41*, e13025. [[CrossRef](#)]
25. Kentish, S.; Ashokkumar, M. The Physical and Chemical Effects of Ultrasound. In *Ultrasound Technologies for Food and Bioprocessing*; Feng, H., Barbosa-Cánovas, G.V., Weiss, J., Eds.; Food Engineering Series; Springer: New York, NY, USA, 2011; pp. 1–12.
26. Chemat, F.; Rombaut, N.; Sicaire, A.-G.; Meullemiestre, A.; Fabiano-Tixier, A.-S.; Abert-Vian, M. Ultrasound assisted extraction of food and natural products. Mechanisms, techniques, combinations, protocols and applications. A review. *Ultrason. Sonochemistry* **2017**, *34*, 540–560. [[CrossRef](#)] [[PubMed](#)]
27. Widmer, V.; Schibli, A.; Reich, E. Quantitative determination of beta-asarone in calamus by high-performance thin-layer chromatography. *J. AOAC Int.* **2005**, *88*, 1562–1567. [[CrossRef](#)] [[PubMed](#)]
28. Pandit, S.; Mukherjee, P.K.; Gantait, A.; Ponnusankar, S.; Bhadra, S. Quantification of alpha-Asarone in Acorus calamus by Validated HPTLC Densitometric Method. *J. Planar Chromatogr.-Mod. TLC* **2011**, *24*, 541–544. [[CrossRef](#)]
29. Hwang, S.H.; Kwon, S.H.; Kang, Y.H.; Lee, J.Y.; Lim, S.S. Rapid High Performance Liquid Chromatography Determination and Optimization of Extraction Parameters of the α -Asarone Isolated from *Perilla frutescens* L. *Molecules* **2017**, *22*, 270. [[CrossRef](#)] [[PubMed](#)]
30. Yu, S.M.; Kim, E.K.; Lee, J.H.; Lee, K.R.; Hong, J. Development of Fingerprints for Quality Control of Acorus species by Gas Chromatography/Mass Spectrometry. *Bull. Korean Chem. Soc.* **2011**, *32*, 1547–1553. [[CrossRef](#)]
31. Meng, X.; Zhao, X.F.; Wang, S.X.; Jia, P.; Bai, Y.J.; Liao, S.; Zheng, X.H. Simultaneous Determination of Volatile Constituents from *Acorus tatarinowii* Schott in Rat Plasma by Gas Chromatography-Mass Spectrometry with Selective Ion Monitoring and Application in Pharmacokinetic Study. *J. Anal. Methods Chem.* **2013**, *2013*, 949830. [[CrossRef](#)]
32. Nandakumar, S.; Menon, S.; Shailajan, S. A rapid HPLC-ESI-MS/MS method for determination of beta-asarone, a potential anti-epileptic agent, in plasma after oral administration of Acorus calamus extract to rats. *Biomed. Chromatogr.* **2013**, *27*, 318–326. [[CrossRef](#)]
33. Hermes, L.; Römermann, J.; Cramer, B.; Esselen, M. Phase II Metabolism of Asarone Isomers In Vitro and in Humans Using HPLC-MS/MS and HPLC-qToF/MS. *Foods* **2021**, *10*, 2032. [[CrossRef](#)]
34. Zhong, S.; Zhang, K.; Shen, L.; Jin, X.; Chen, R.; Shen, W. Iron (III)-mediated degradation of α -asarone and characterization of its major degradation products by UPLC-MS/MS and NMR. *Pharmazie* **2021**, *76*, 588–593. [[CrossRef](#)]
35. Ying, X.H.; Pei, Y.; Liu, M.Y.; Ding, G.Y.; Jiang, M.; Liang, Q.L.; Wang, Y.M.; Bai, G.; Luo, G.A. Discrimination and quantification analysis of Acorus calamus L. and Acorus tatarinowii Schott with near-infrared reflection spectroscopy. *Anal. Methods* **2014**, *6*, 4212–4218. [[CrossRef](#)]
36. So, G.C.; Macdonald, D.G. Kinetics of oil extraction from canola (rapeseed). *Can. J. Chem. Eng.* **1986**, *64*, 80–86. [[CrossRef](#)]
37. Takeuchi, T.M.; Pereira, C.G.; Braga, M.E.M.; Maróstica, M.R.; Leal, P.F.; Meireles, M.A.A. Low-Pressure Solvent Extraction (Solid-Liquid Extraction, Microwave Assisted, and Ultrasound Assisted) from Condimentary Plants. In *Extracting Bioactive Compounds for Food Products*; Meireles, M.A.A., Ed.; CRC Press: Boca Raton, FL, USA, 2008.
38. β -Asarone. In Cayman Chemical. Available online: [https://www.caymanchem.com/product/11682/\\$\upbeta\\$-Asarone](https://www.caymanchem.com/product/11682/\upbeta-Asarone) (accessed on 14 July 2022).
39. Ashokkumar, M.; Mason, T.J. Sonochemistry. In *Kirk-Othmer Encyclopedia of Chemical Technology*; John Wiley & Sons, Inc.: Hoboken, NJ, USA, 2007.

40. Fu, X.; Belwal, T.; Cravotto, G.; Luo, Z. Sono-physical and sono-chemical effects of ultrasound: Primary applications in extraction and freezing operations and influence on food components. *Ultrason. Sonochemistry* **2020**, *60*, 104726. [[CrossRef](#)] [[PubMed](#)]
41. Lv, S.; Taha, A.; Hu, H.; Lu, Q.; Pan, S. Effects of Ultrasonic-Assisted Extraction on the Physicochemical Properties of Different Walnut Proteins. *Molecules* **2019**, *24*, 4260. [[CrossRef](#)] [[PubMed](#)]
42. Tao, Y.; Sun, D.-W. Enhancement of Food Processes by Ultrasound: A Review. *Crit. Rev. Food Sci. Nutr.* **2015**, *55*, 570–594. [[CrossRef](#)]
43. Meullemiestre, A.; Breil, C.; Abert-Vian, M.; Chemat, F. Microwave, ultrasound, thermal treatments, and bead milling as intensification techniques for extraction of lipids from oleaginous *Yarrowia lipolytica* yeast for a biojetfuel application. *Bioresour. Technol.* **2016**, *211*, 190–199. [[CrossRef](#)]
44. Veillet, S.; Tomao, V.; Chemat, F. Ultrasound assisted maceration: An original procedure for direct aromatisation of olive oil with basil. *Food Chem.* **2010**, *123*, 905–911. [[CrossRef](#)]